

A Numerical Study on the Rotational Motion of an  
Axisymmetric Particle in a Viscous Fluid

---

A Thesis

Presented to

The Faculty of the Graduate School  
University of Missouri-Columbia

---

In Partial Fulfillment  
of the Requirement for the Degree  
Master of Science

---

By

Rong-Jin Leu

Dr. Paul C.-H. Chan

Thesis Supervisor

December 1983

The undersigned, appointed by the Dean of the Graduate Faculty,  
have examined a thesis entitled

A Numerical Study on the Rotational Motion of an Axisymmetric Particle  
in a Viscous Fluid

presented by

Leu, Rong-Jin  
a candidate for the degree of

Master of Science  
and hereby certify that in their opinion it is worthy of acceptance.

Paul C. Chan

David B. Reitzeloff

Sunderban Loyalka

## ACKNOWLEDGEMENTS

The author wishes to express his sincere appreciation to his advisor, Dr. Paul C.-H. Chan, for his sustaining guidance and advice during the course of his studies and in the preparation of this thesis. Grateful appreciation is also extended to author's committee members: Drs. David G. Retzloff and Sudarshan K. Loyalka, for their continuing support and advice. Special acknowledgment is extended to the author's parents for their continued encouragement and understanding during the course of this study.

## TABLES OF CONTENTS

Acknowledgements

List of Tables

List of Figures

Chapter	Page
1.0 Introduction.....	1
2.0 Mathematical Formulation.....	5
2.1 Green's Function Approach.....	6
2.2 Asymptotic Solution.....	9
3.0 Computer Program.....	12
3.1 Thin Disc.....	14
3.2 Finite Disc.....	22
4.0 Applications.....	32
4.1 Velocity Field.....	32
4.2 Torque Comparison.....	33
5.0 Recommendations and Conclusions.....	37
6.0 References.....	38

### Appendices

A. FORTRAN program for calculating the numerical stress distribution and torque of the rotating thin disc.....	40
B. FORTRAN program for calculating the numerical stress distribution and torque of the rotating finite disc.....	44

## LIST OF TABLES

	Page
1. Comparison of Calculated $f$ and $T$ with Theoretical Values for the Rotation of Thin Disc for $N=10$ .....	19
2. Comparison of Calculated $f$ and $T$ with Theoretical Values for the Rotation of Thin Disc for $N=100$ .....	20
3A. Calculated $f$ and $T$ for the Rotation of Finite Discs for $N=10$ .....	26
3B. Calculated $f$ and $T$ for the Rotation of Finite Discs for $N=10$ .....	27
4A. Calculated $f$ and $T$ for the Rotation of Finite Discs for $N=50$ .....	28
4B. Calculated $f$ and $T$ for the Rotation of Finite Discs for $N=50$ .....	29
5. Calculated Values of $f$ as a Function of $m, n$ ( $\alpha=1, N=10$ ).....	31

## LIST OF FIGURES

	Page
1. Velocity Field due to the Rotation of a Thin Disc ( $\alpha=0$ ).....	34
2. Velocity Field due to the Rotation of a Finite Disc ( $\alpha=1$ ).....	35
3. The Comparison of Numerical Results with Equation (2.23).....	36

## 1.0 INTRODUCTION

The motion of a single particle in an inertialess unbounded Newtonian fluid has been studied for more than 100 years. The applications of such problems in industry are: the transport of slurries in pulp processing, the extrusion of molten plastics, the motion of oil droplets in polymeric fluids during oil recovery, the manufacture of films or magnetic tapes, and so forth. Similar problems are also encountered in the study of natural substances such as atmospheric aerosols. For the past few years, environmental engineers have shown great interest in the measurement of the particle size distribution and the design of sampling instruments for these aerosols, but they all met with difficulties due to a lack of basic understanding about their hydrodynamic behavior in various external fields. Thus, a fundamental understanding of this problem is clearly useful and important to making progress in many modern technological areas.

Starting from the early works of Stokes (1851) and Kirchhoff (1869) on the slow translation and rotation of a solid sphere in a Newtonian fluid, more recent investigators have included additional effects such as inertia, non-Newtonian fluid properties and external boundaries. These are interesting problems in their own right, and extensive review articles have been written on these subject areas (Caswell

1977, Leal 1979,1980, Brunn 1980). Quite often, the solution procedure for these problems involves the use of perturbation methods, which account for these additional effects by assuming that they are small in relation to the primary flow. Other investigators have considered the motion of nonspherical rigid particles in unbounded Stokes flow. Here, the methods that are used can be roughly classified into three categories: (1) the method of separation of variables, which may be labeled 'exact', for particles with 'regular' geometries such as ellipsoids or spheroids (Oberbeck 1876, Jeffrey 1915,1922, Payne and Pell 1960), spherical caps or lenses (Payne and Pell 1960, Collins 1963, Dorrepaal, O'Neill and Ranger 1976), thin discs (Ray 1936, Gupta 1957), toroids (Kanwal 1961, Majumdar and O'Neill 1977, Goren and O'Neill 1980), and two spheres either at a finite separation (Jeffrey 1915, Stimson and Jeffrey 1926) or in contact with each other (Cooley and O'Neill 1969); (2) the method of singularities for long slender bodies (Burgers 1938, Broersma 1960, Batchelor 1970, Tillett 1970 and Cox 1970, 1971); and (3) the numerical methods for 'irregular' geometries (Youngren and Acrivos 1975, Gluckman, Weinbaum and Pfeffer 1972, Bowen and Masliyah 1973). The technique that we will use is of the last group.

In this thesis, we are interested in solving the problem of the slow axial rotation of a single, finite axisymmetric particle in a Newtonian fluid. We will use the method of

Green's functions to develop a general solution procedure, which results in an integral equation to be solved, in general, by numerical computations. Our calculations are to be compared with known results for the particular case of a thin disc (Ray 1936), and then the problem of a finite cylinder will be considered.

It should be noted that the integral equation which is obtained can easily be replaced by a set of algebraic equations, which may then be inverted by standard methods. As we shall see in the following paragraphs, very high accuracy can be achieved even with only minimal computer effort, despite the fact that an integral equation of the first kind (which this one is) is well known to be often ill-posed. Thus, our procedure is far superior to both the finite difference and the finite element methods, which, as pointed out by Gluckman, Weinbaum and Pfeffer (1973) and by Youngren and Acrivos (1975), are extremely unsuitable for problems of this nature since the domain of interest extends to infinity. In fact, similar numerical techniques have been applied to other problems areas in physics as well, such as elastostatics in three dimensions (Cruse 1969), heat conduction in an anisotropic medium (Chang, Kang and Chen, 1973) and potential flow past arbitrary bodies (Smith and Hess 1966) or through an orifice (Hunt 1968). In addition, for numerous problems involving an infinitesimally thin disc where the cumbersome method of dual integral equations must

frequently be used, (such as in the calculation of the surface charge density and potential in an external electrostatic field (Copson 1945)), our method can obviously be applied to extend the results to a finite disc. Other types of problems in Stokes flow, such as the axisymmetric motion of an arbitrary particle, can also be treated by similar procedures, and our calculations in this thesis will be the starting point for later work in this area.

## 2.0 MATHEMATICAL FORMULATION

The method that we will follow is similar to that in Shail (1979). A single, finite rigid axisymmetric particle rotates slowly with angular velocity  $\omega$  about its own axis in an otherwise motionless unbounded Newtonian fluid. The particle surface is denoted as  $S$ . The cylindrical coordinate system  $(\rho, \theta, z)$  is chosen with  $z$  coinciding with the particle axis. By neglecting the inertia terms (i.e. assuming small Reynold's number), it is easily shown from the equation of motion that the only nonzero velocity component is in the  $\theta$ -direction, which we denote as  $v$ . It satisfies

$$\frac{\partial^2 v}{\partial \rho^2} + \frac{1}{\rho} \frac{\partial v}{\partial \rho} + \frac{\partial^2 v}{\partial z^2} - \frac{v}{\rho^2} = 0 \quad (2.1)$$

The boundary conditions are

$$\begin{aligned} v &\longrightarrow 0 && \text{as } |r| = (\rho^2 + z^2)^{1/2} \longrightarrow \infty \\ v &= 0 && \text{on } S \end{aligned} \quad (2.2)$$

A transformation first used by Jeffrey (1915) is introduced to convert equation (2.1) into the Laplace equation. Thus, we define

$$w = v \cos \theta \quad (2.3)$$

By substituting and using equation (2.1), it can be shown that  $w$  is a harmonic function, that is,

$$\nabla^2 w = 0 \quad (2.4)$$

The boundary conditions now become

$$w \longrightarrow 0 \quad \text{as } |\underline{r}| \longrightarrow \infty \quad (2.5)$$

$$w = \rho \cos \theta \quad \text{on } S$$

Since  $S$  is not represented by a single coordinate surface (even in cylindrical coordinates), it is virtually impossible to satisfy the above boundary conditions by applying the usual method of separation of variables, and hence some other solution procedure must be used.

### 2.1 Green's Function Approach

We consider a Green's function  $G(\underline{r}; \underline{r}')$  which satisfies

$$\nabla'^2 G = -4\pi\delta(\underline{r} - \underline{r}') \quad (2.6)$$

By applying the divergence theorem to the integral of  $w'\nabla'^2 G$  over the entire domain of fluid, we obtain

$$w(\underline{r}) = \frac{1}{4\pi} \int_{S'} \left[ w' \frac{\partial G(\underline{r}; \underline{r}')}{\partial n'} - G(\underline{r}; \underline{r}') \frac{\partial w'}{\partial n'} \right] dS' \quad (2.7)$$

Here,  $n$  is directed into the fluid, and all primed quantities are written by using the dummy variables  $\rho'$ ,  $\theta'$ ,  $z'$ .

The first term on the R.H.S. of equation (2.7) can be simplified by applying equation (2.5) and using the identity

$$\int_{S'} \rho' \cos \theta' \frac{\partial G(\underline{r}; \underline{r}')}{\partial n'} dS' = \int_{S'} G(\underline{r}; \underline{r}') \frac{\partial (\rho' \cos \theta')}{\partial n'} dS' \quad (2.8)$$

Combining (2.7), (2.8) and (2.3), we finally obtain

$$w(\underline{r}) = \frac{-1}{4\pi} \int_{S'} G(\underline{r}; \underline{r}') \frac{\partial}{\partial n'} \left( \frac{v'}{\rho'} \right) \rho' \cos \theta' dS' \quad (2.9)$$

We only need to consider the coefficient of  $\cos(\theta - \theta')$  in the Fourier expansion of  $G(\underline{r}; \underline{r}')$ , which we denote as  $G_1(\rho, z; \rho', z')$ , since all other terms integrate to zero. Thus

$$v \cos \theta = \frac{-1}{4\pi} \int_{S'} G_1(\rho, z; \rho', z') \cos(\theta - \theta') \frac{\partial}{\partial n'} \left( \frac{v'}{\rho'} \right) \rho' \cos \theta' dS' \quad (2.10)$$

After integrating over  $\theta'$ , we obtain

$$v = \frac{-1}{4} \int_{C'} G_1(\rho, z; \rho', z') \frac{\partial}{\partial n'} \left( \frac{v'}{\rho'} \right) \rho'^2 dl' \quad (2.11)$$

where C is the bounding curve of S along a meridian plane. The Green's function is known to be

$$G_1(\rho, z; \rho', z') = 2 \int_0^\infty J_1(\lambda \rho) J_1(\lambda \rho') e^{-\lambda |z-z'|} d\lambda \quad (2.12)$$

Application of (2.2) to (2.11) will result in a Fredholm

integral equation of the first kind and the value of  $\rho \frac{\partial v}{\partial n} (-)$

can be obtained. It should be noted that this function represents the stress distribution on the particle surface, and will be denoted henceforth as  $\sigma(\rho, z)$ . The dimensionless torque is

$$\begin{aligned} T &= \int_S \rho \sigma(\rho, z) dS \\ &= 2\pi \int_C \rho^2 \sigma(\rho, z) dl \end{aligned} \quad (2.13)$$

We may now consider the specific case of a rigid circular cylinder with radius a and length 2b. The aspect ratio  $\alpha$  is defined as b/a. Applying the boundary conditions (2.2), equation (2.11) now becomes

$$\rho = -\frac{1}{4} \left\{ \int_0^1 \left[ G_1(\rho, \alpha; \rho', \alpha) + G_1(\rho, \alpha; \rho', -\alpha) \right] \sigma'(\rho', \alpha) \rho' d\rho' \right.$$

$$+ \left. \int_0^{\alpha} [G_1(\rho, \alpha; 1, z') + G_1(\rho, \alpha; 1, -z')] \sigma'(1, z') dz' \right\}$$

$$(0 \leq \rho < 1) \quad (2.14)$$

$$1 = -\frac{1}{4} \left\{ \int_0^1 [G_1(1, z; \rho', \alpha) + G_1(1, z; \rho', -\alpha)] \sigma'(\rho', \alpha) \rho' d\rho' \right.$$

$$+ \left. \int_0^{\alpha} [G_1(1, z; 1, z') + G_1(1, z; 1, -z')] \sigma'(1, z') dz' \right\}$$

$$(-\alpha < z < \alpha) \quad (2.14)$$

## 2.2 Asymptotic Solution

An asymptotic analysis may be applied to the integral equation (2.14) for very large or very small values of  $\alpha$ . Though it is extremely difficult to carry this to completion, the leading terms are shown to be correct in the two limiting cases:

(i) Infinitesimally Thin Disc:

For  $\alpha \ll 1$ , equation (2.14) reduces to

$$\rho = -\frac{1}{2} \int_0^1 G_1(\rho, 0; \rho', 0) \sigma_0'(\rho', 0) \rho' d\rho'$$

$$(0 \leq \rho < 1) \quad (2.15)$$

where from equation (2.12)

$$G_1(\rho, 0; \rho', 0) = 2 \int_0^{\infty} J_1(\lambda \rho) J_1(\lambda \rho') d\lambda \quad (2.16)$$

The solution may be obtained by standard methods:

$$\sigma_0'(\rho', 0) = -\frac{4}{\pi} \frac{\rho'}{(1-\rho'^2)^{1/2}} \quad (2.17)$$

Substituting (2.17) into (2.11) and (2.13), we get

$$v_0 = \frac{4}{\pi} \int_0^\infty \left( \frac{\sin \lambda}{\lambda^2} - \frac{\cos \lambda}{\lambda} \right) J_1(\lambda \rho) e^{-\lambda |z|} d\lambda \quad (2.18)$$

$$T_0 = -(32/3)$$

which agree with the previous results for the infinitesimal-ly thin disc (Ray, 1936).

(ii) Infinitely Long Rod:

For  $\alpha \gg 1$ , (2.14) reduces to

$$1 = -\frac{1}{4} \int_{-\infty}^{\infty} G_1(1, z; 1, z') \sigma'(1, z') dz' \quad (2.19)$$

( all z )

where

$$G_1(1, z; 1, z') = 2 \int_0^\infty [J_1(\lambda)]^2 e^{-\lambda |z-z'|} d\lambda \quad (2.20)$$

Further simplifications yield

$$\sigma'(1, z') = -2 \quad (2.21)$$

Substituting (2.21) into (2.11), we obtain the result

$$v = \frac{1}{\rho} \tag{2.22}$$

$$T = -8\pi\alpha$$

which is clearly correct.

By adding (2.18) and (2.22), an expression is obtained which is approximately correct in the two limits

$$T = -\frac{32}{3} \left( 1 + \frac{3}{4} \pi \alpha \right) \tag{2.23}$$

We will use this ad hoc equation for future comparisons with our numerical results.

### 3.0 Computer Program

As mentioned in the previous paragraphs, an exact analytical treatment of equation (2.11) subject to boundary conditions (2.2) is not possible for arbitrary values of  $\alpha$ , and thus a numerical procedure will be used. Our method follows closely that of Youngren and Acrivos (1975). For problems where  $\sigma(\rho, z)$  is always continuous on  $S$  (usually this happens if and only if the rigid particle's surface is everywhere smooth in some sense), the most obvious procedure is to divide  $C$  into  $N$  elements,  $\delta_j$ , and replace equation (2.11) by

$$v = -\frac{1}{4} \sum_{j=1}^N \sigma(\bar{\rho}_j, \bar{z}_j) \int_{\delta_j} G_1(\rho, z; \rho', z') \rho' dl' \quad (3.1)$$

where  $\sigma(\bar{\rho}_j, \bar{z}_j)$  is the value of  $\sigma$  evaluated at the center  $(\bar{\rho}_j, \bar{z}_j)$  of the interval  $\delta_j$ . By a Taylor's series expansion of  $\sigma$  in equation (2.11), it is easily seen that this approximation has a numerical error which is  $O(\epsilon)$ , where  $\epsilon$  is the maximum length of the line elements  $\delta_j$ , i.e. it is formally a first-order method. Since the integrand in equation (3.1) is a known function, it can in principle be evaluated to any degree of accuracy.  $G_1(\rho, z; \rho', z')$  can be obtained analytically in closed form as follows: from p.389 of Watson (1966)

$$\int_0^{\infty} e^{-at} J_{\nu}(bt) J_{\nu}(ct) dt = \frac{1}{\pi\sqrt{bc}} Q_{\nu-1/2} \left( \frac{a^2+b^2+c^2}{2bc} \right) \quad (3.2)$$

Substituting back into equation (2.12) which then becomes

$$G_1(\rho, z; \rho', z') = \frac{2}{\pi\sqrt{\rho\rho'}} Q_{1/2} \left[ \frac{(z-z')^2 + \rho^2 + \rho'^2}{2\rho\rho'} \right] \quad (3.3)$$

From equation (8.13.7) of Abramowitz and Stegun (1970)

$$Q_{1/2}(Z) = Z \left( \frac{2}{Z+1} \right)^{1/2} K \left[ \left( \frac{2}{Z+1} \right)^{1/2} \right] - [2(Z+1)]^{1/2} E \left[ \left( \frac{2}{Z+1} \right)^{1/2} \right] \quad (3.4)$$

where  $K$  and  $E$  are the elliptic integrals. However, it appears that this equation is inconsistent with the definitions of  $K$  and  $E$  which appear in Chapter 17 of Abramowitz and Stegun (1970), and will result in an incorrect numerical value for  $Q_{1/2}(Z)$ . The correct expression should be

$$Q_{1/2}(Z) = Z \left( \frac{2}{Z+1} \right)^{1/2} K \left( \frac{2}{Z+1} \right) - [2(Z+1)]^{1/2} E \left( \frac{2}{Z+1} \right) \quad (3.4a)$$

For our numerical calculations, we shall use the polynomial approximations for  $K$  and  $E$  that appear in Chapter 17 [cf. equation (17.3.34) and equation (17.3.36) of Abramowitz and Stegun (1970)]. Moreover, it can be seen that  $Q_{1/2}(Z)$  exhibits a logarithmic singularity when the modulus of the elliptic function  $K$  is equal to 1, i.e., the term  $G_1(\rho, z, \rho', z')$  is singular when  $\rho = \rho'$  and  $z = z'$ , as expected. Therefore, the

algorithm that is used must take this into account. By applying boundary condition (2.2) to equation (3.1) at the center of each of the N subintervals, we obtain a set of N algebraic equations, which are

$$\bar{\rho}_i = -\frac{1}{4} \sum_{j=1}^N \sigma(\bar{\rho}_j, \bar{z}_j) \int_{\delta_j} G_1(\bar{\rho}_i, \bar{z}_i; \rho', z') \rho' dl' \quad (3.5)$$

$i=1, \dots, N$

It remains to solve this set of equations and obtain the unknown function  $\sigma$  for any aspect ratio  $\alpha$ .

Our numerical experiment will thus consist of two parts. First, an algorithm is developed and applied to the case of an infinitesimally thin disc. Here, we can improve on the numerical scheme, as well as obtain more accurate error estimates of our calculated results, by direct comparisons with the theoretical prediction of equation (2.17) and (2.18). The algorithm is then applied to the case of a finite cylinder.

### 3.1 Thin Disc

A first attempt here to apply boundary condition (2.2) to equation (3.1), and then invert the resulting matrix equation by Gaussian elimination, results in a stress

distribution which compares very poorly with (2.17), especially near the edge of the disc, i.e. when  $\rho$  approaches unity. In retrospect this is, of course, to be expected, since the stress distribution  $\sigma(\rho, 0)$  is singular near the edge, and hence the approximate equation (3.1) should not be valid. The difficulty can be circumvented easily, if we first anticipate the stress distribution (2.17), and use an alternative approximation for equation (2.15)

$$\bar{\rho}_i = -\frac{1}{2} \sum_{j=1}^N f(\bar{\rho}_j) \int_{\delta_j} G_1(\bar{\rho}_i, 0; \rho', 0) \frac{\rho'}{(1-\rho'^2)^{1/2}} d\rho' \quad i=1, \dots, N \quad (3.6)$$

where

$$f(\rho) = \sigma(\rho, 0) (1-\rho^2)^{1/2} \quad (3.7)$$

Clearly  $f(\rho)$  will be continuous for  $\rho$  between 0 and 1. Also, we will expect the improper integral in equation (3.6) (the integrand is singular at  $\rho' = \bar{\rho}_i$  and at  $\rho' = 1$ ) to be finite, since the original integral in equation (2.15) is known to be also finite. It remains now to calculate this line integral as accurately as possible, and then invert the resulting set of  $N \times N$  matrix equations. Applying equation (3.3), we obtain

$$\int_{\delta_j} G_1(\rho, 0; \rho', 0) \frac{\rho'}{(1-\rho'^2)^{1/2}} d\rho' = \frac{2}{\pi} \int_{\delta_j} \left(\frac{\rho'}{\rho}\right)^{1/2} \frac{1}{(1-\rho'^2)^{1/2}} Q_{1/2}\left(\frac{\rho^2 + \rho'^2}{2\rho\rho'}\right) d\rho' \quad (3.8)$$

The singularity at  $\rho'=1$  (which is more severe) can be removed by simply substituting  $\rho' = \sin\theta$  and  $\bar{\rho}_j = \sin\varphi_j$  into equation (3.6). Thus equation (3.6) easily turns out to be

$$\sin\varphi_j = \sum_{j=1}^N \frac{1}{2} f(\sin\varphi_j) \int_{\delta_j\pi} \frac{2 \sin\theta}{\sin\varphi_j} Q_{1/2} \left( \frac{\sin^2\varphi_j + \sin^2\theta}{2\sin\varphi_j \sin\theta} \right) d\theta \quad (3.9)$$

$i=1, \dots, N$

Although a singularity still exists in equation (3.9) when  $\delta_j$  includes the point  $\theta = \varphi_j$ , this weak logarithmic singularity does not pose any great difficulties and the integral may be evaluated accurately by most standard numerical integration routines, so long as the point  $\theta = \varphi_j$  is avoided, e.g. for  $\theta < \varphi_j$ , integrate up to  $\theta = \varphi_j - \kappa$ , where  $\kappa$  is a small number, with the error estimated analytically. However, a more elegant procedure is to note that

$$\lim_{\theta \rightarrow \varphi_j} \left( \frac{\sin\theta}{\sin\varphi_j} \right)^{1/2} Q_{1/2} \left( \frac{\sin^2\varphi_j + \sin^2\theta}{2\sin\varphi_j \sin\theta} \right) = \ln \frac{8 \tan\varphi_j}{|\theta - \varphi_j|} - 2 \quad (3.10)$$

and hence the singularity at  $\theta = \varphi_j$  may be 'removed' by adding to, and subtracting from, the integrand of equation (3.9) this same term. Thus, we obtain

$$\sin\varphi_j = \frac{1}{\pi} \sum_{j=1}^N f(\sin\varphi_j) \left\{ \int_{\delta_j} \left[ \left( \frac{\sin\theta}{\sin\varphi_j} \right)^{1/2} Q_{1/2} \left( \frac{\sin^2\varphi_j + \sin^2\theta}{2\sin\varphi_j \sin\theta} \right) + \ln|\theta - \varphi_j| - \ln(8\tan\varphi_j) + 2 \right] d\theta - \int_{\delta_j} \left[ \ln|\theta - \varphi_j| - \ln(8\tan\varphi_j) + 2 \right] d\theta \right\}$$

$$i=1, \dots, N \quad (3.11)$$

The second integral in equation (3.11) is easily evaluated for any interval  $\delta_j$ . For the first integral, the integrand is now always bounded (although its first derivative does not always exist), hence the numerical calculation poses no great difficulties. The unknown function  $f$  can now be obtained by solving the system of  $N \times N$  matrix equations by standard Gaussian elimination routines.

The numerical value of the torque follows from (2.13), and can be written as

$$T = 2 (2\pi) \int_0^1 \rho^2 \sigma(\rho, 0) d\rho \quad (3.12)$$

Again, by replacing  $\sigma(\rho, 0)$  with  $f(\rho)$  and approximating the integral with an algebraic sum, we obtain

$$T = 4\pi \sum_{j=1}^N f(\rho_j) \int_{\delta_j} \rho^2 (1-\rho^2)^{-1/2} d\rho \quad (3.13)$$

where the integral can be evaluated analytically for any subinterval  $\delta_j$ . Therefore, the torque can be calculated easily as long as the stress distribution is known.

We have listed our computer program in Appendix A. Of special interest are the following details:

(i) The program is written in double precision throughout.

As expected with numerical problems of this nature, convergence cannot be attained by using single precision arithmetic.

(ii) The intervals  $\delta_j$  ( $j=1, \dots, N$ ) are arbitrarily chosen to be of equal length  $\pi/(2N)$ . (Recall that the independent variable  $\theta$  goes from 0 to  $\pi/2$ ). No attempt is made to optimize the interval sizes.

(iii) Two subroutines are called from the IMSL library, which is available in Fortran IV from the UMC computing facilities. These are: DCADRE, which computes an integral by Romberg integration with extrapolation, and LEQT2F, which performs Gaussian elimination (Crout algorithm) with equilibration, partial pivoting, and iterative improvement if necessary.

Our numerical results are listed in Table 1 ( $N=10$ ) and Table 2 ( $N=100$ ).

TABLE 1  
 COMPARISON OF CALCULATED  $f$  AND  $T$  WITH THEORETICAL  
 VALUES FOR THE ROTATION OF THIN DISC FOR  $N=10$

		Calculated values	Theoretical values	Percentage error
$i$	$\phi_j$	Stress distribution $f$		
1	4.5°	-0.10619	-0.09990	6.2968
2	13.5°	-0.29753	-0.29724	0.1010
3	22.5°	-0.48783	-0.48724	0.1181
4	31.5°	-0.66594	-0.66527	0.1020
5	40.5°	-0.82771	-0.82691	0.0979
6	49.5°	-0.96911	-0.96818	0.0962
7	58.5°	-1.08665	-1.08561	0.0954
8	67.5°	-1.17744	-1.17632	0.0951
9	76.5°	-1.23923	-1.23806	0.0945
10	85.5°	-1.27053	-1.26932	0.0954
		Torque $T$		
		-10.666	-10.667	0.0064

TABLE 2  
 COMPARISON OF CALCULATED  $f$  AND  $T$  WITH THEORETICAL  
 VALUES FOR THE ROTATION OF THIN DISC FOR  $N=100$

		Calculated values	Theoretical values	Percentage error
$i$	$\varphi_i$	Stress distribution $f$		
1	0.45°	-0.01048	-0.00999	4.7561
5	4.05°	-0.08993	-0.08993	0.004563
10	8.55°	-0.18929	-0.18929	0.001630
20	17.55°	-0.38393	-0.38393	0.000953
30	26.55°	-0.56911	-0.56911	0.000878
40	35.55°	-0.74029	-0.74027	0.000861
50	44.55°	-0.89323	-0.89322	0.000866
60	53.55°	-1.02417	-1.02417	0.000861
70	62.55°	-1.12990	-1.12989	0.000859
80	71.55°	-1.20781	-1.20779	0.000867
90	80.55°	-1.25597	-1.25596	0.000880
100	89.55°	-1.27337	-1.27320	0.008571
		Torque $T$		
		-10.667	-10.667	-0.000172

As we observed at the beginning of this chapter, our numerical approximation is, formally, only a first-order method. However, from Table 1 and 2, it is clear that the actual percentage errors of the calculated stress distribution and torque are much smaller than what may be expected. Since a tenfold increase in  $N$  reduces the relative error by roughly 100 times, we estimate that the numerical procedure is actually second-order, i.e.

$$\text{error} = \frac{f_{\text{calc.}} - f_{\text{exact}}}{f_{\text{exact}}} = \frac{C}{N^2} \quad (3.14)$$

$C$  will depend strongly on position. Quite surprisingly, the error is large only near the center of the disc. One plausible explanation here is that the numerical approximation (3.6) is poorest when  $\rho$  is small, since  $f(\rho)$  itself will be a small number and therefore the leading term in its Taylor's series expansion will not numerically dominate the next term. We should also note that this large error in  $f$  at small  $\rho$  does not contribute significantly to the numerical errors of the macroscopic properties such as the torque. In fact, the percentage error of  $T$  is an order of magnitude smaller than that of  $f$ . Since the torque is given by equation (3.13), this effective improvement in accuracy must be due to cancellation of any systematic numerical errors that were introduced by equation (3.6). In view of the superior accuracy of our algorithm applied to the test

case, we are now confident to proceed to the problem of a finite circular disc.

### 3.2 Finite Disc

In this case, no analytical solution is possible at present, and we must follow the same numerical procedure as outlined in section 3.1 to find the stress distribution and the torque for arbitrary values of the aspect ratio  $\alpha$ .

First, we attempt to replace (2.14) with an algebraic equation analogous to (3.6) with the condition that the unknown function which appears outside the line integral over  $\delta_j$  must be continuous. Although the asymptotic behavior of the stress distribution  $\sigma(\rho, z)$  as we approach the edge of the finite disc cannot be determined a priori for any arbitrary  $\alpha$ , it is intuitively obvious that the singularity for intermediate values of  $\alpha$  will not be as severe as for the limiting cases of large and small  $\alpha$ . Thus, we hypothesize that the functions

$$\begin{aligned} f(\rho, \alpha) &= \sigma(\rho, \alpha) (1-\rho^2)^{1/2} \\ f(1, z) &= \sigma(1, z) (\alpha^2-z^2)^{1/2} \end{aligned} \tag{3.15}$$

will work, i.e.  $f(\rho, \alpha), f(1, z)$  will both be continuous on the particle surface. A more accurate estimate of the strength of the singularity will be attempted later. Dividing the

interval  $0 < \rho < 1$  into  $N$  subintervals  $\delta_j$  and the interval  $0 < z < \alpha$  into  $N$  subintervals  $\epsilon_j$ , and substituting (3.15) into (2.14), we obtain after carrying out the usual manipulations

$$\begin{aligned} \bar{\rho}_j = & -\frac{1}{4} \left\{ \sum_{j=1}^N f(\bar{\rho}_j, \alpha) \int_{\delta_j} \left[ G_1(\bar{\rho}_j, \alpha; \rho', \alpha) + G_1(\bar{\rho}_j, \alpha; \rho', -\alpha) \right] \frac{\rho'}{(1-\rho'^2)^{1/2}} d\rho' \right. \\ & \left. + \sum_{j=1}^N f(1, \bar{z}_j) \int_{\epsilon_j} \left[ G_1(\bar{\rho}_j, \alpha; 1, z') + G_1(\bar{\rho}_j, \alpha; 1, -z') \right] \frac{1}{(\alpha^2 - z'^2)^{1/2}} dz' \right\} \\ 1 = & -\frac{1}{4} \left\{ \sum_{j=1}^N f(\bar{\rho}_j, \alpha) \int_{\delta_j} \left[ G_1(1, \bar{z}_j; \rho', \alpha) + G_1(1, \bar{z}_j; \rho', -\alpha) \right] \frac{\rho'}{(1-\rho'^2)^{1/2}} d\rho' \right. \\ & \left. + \sum_{j=1}^N f(1, \bar{z}_j) \int_{\epsilon_j} \left[ G_1(1, \bar{z}_j; 1, z') + G_1(1, \bar{z}_j; 1, -z') \right] \frac{1}{(\alpha^2 - z'^2)^{1/2}} dz' \right\} \\ & i=1, \dots, N \qquad (3.16) \end{aligned}$$

This is a set of  $2N \times 2N$  matrix equations which can be solved as before. The integrals are simplified by letting  $\rho' = \sin\theta$ ,  $\bar{\rho}_j = \sin\varphi_j$ ,  $z' = \alpha \sin\beta$  and  $\bar{z}_j = \alpha \sin\gamma_j$ . Finally, the logarithmic singularity at the point  $\theta = \varphi_j$ ,  $\beta = \gamma_j$  can be removed by the same procedure as in the previous section, which allows the line integrals to be calculated numerically. The resulting system is again solved by Gaussian elimination.

From the calculated values of  $f(\sin\varphi_j, \alpha)$  and  $f(1, \alpha \sin\gamma_j)$ , we can also calculate the torque using equation (2.13)

$$T = 4\pi \left[ \sum_{j=1}^N f(\bar{\rho}_j, \alpha) \int_{\delta_j} \rho^2 (1-\rho^2)^{-1/2} d\rho + \sum_{j=1}^N f(1, \bar{z}_j) \int_{\epsilon_j} (\alpha^2 - z^2)^{-1/2} dz \right] \quad (3.17)$$

Our computer program for this problem is listed in Appendix B. The numerical results for the stress distribution  $f$  and torque  $T$  are shown in Tables 3 and 4.

We note that all the results obtained so far follow trends that are to be intuitively expected. Of special interest, however, is the fact that the torque per unit length for the case of  $\alpha=100$  is found to be larger than that predicted by the asymptotic theory, i.e. equation (2.22). This result is qualitatively correct, since the asymptotic theory does not take the contribution of the flat ends or the singularity at the corners into account. It should also be noted that Chwang and Wu (1974) have previously obtained analytically the torque on a rotating axisymmetric prolate body with a 'smooth' shape, and when their results are considered in the limit of a long slender body, it is found that the torque per unit length is less than that of equation (2.22). There is no contradiction between the differing results, however, since a long rod with rounded ends will have no singularities and the contribution to the torque from those rounded ends will actually be even smaller

than when a uniform radius is assumed, as is inherently done in deriving equation (2.22).

TABLE 3A

CALCULATED  $f$  AND  $T$  FOR THE ROTATION OF FINITE DISCS FOR  $N=10$ 

$\gamma_j=90^\circ$ (flat end, $z=\alpha$ )		$\alpha=0.01$	$\alpha=0.1$	$\alpha=1$
$i$	$\varphi_j$	stress distribution $f$		
1	4.5°	-0.1056	-0.1007	-0.0948
2	13.5°	-0.2938	-0.2816	-0.2645
3	22.5°	-0.4812	-0.4599	-0.4307
4	31.5°	-0.6557	-0.6235	-0.5813
5	40.5°	-0.8123	-0.7664	-0.7101
6	49.5°	-0.9459	-0.8816	-0.8100
7	58.5°	-1.0503	-0.9604	-0.8726
8	67.5°	-1.1158	-0.9892	-0.8856
9	76.5°	-1.1239	-0.9432	-0.8362
10	85.5°	-0.9232	-0.7066	-0.5507

TABLE 3B

CALCULATED  $f$  AND  $T$  FOR THE ROTATION OF FINITE DISCS FOR  $N=10$ 

$\varphi_j = 90^\circ$ (curved side, $\rho=1$ )		$\alpha=0.01$	$\alpha=0.1$	$\alpha=1$
$i$	$\gamma_j$	stress distribution $f$		
11	85.5°	-0.0089	-0.0841	-0.5796
12	76.5°	-0.0538	-0.2341	-0.9943
13	67.5°	-0.0736	-0.2811	-1.2436
14	58.5°	-0.0872	-0.3165	-1.4736
15	49.5°	-0.0968	-0.3452	-1.6805
16	40.5°	-0.1039	-0.3689	-1.8624
17	31.5°	-0.1091	-0.3878	-2.0151
18	22.5°	-0.1127	-0.4020	-2.1340
19	13.5°	-0.1150	-0.4114	-2.2155
20	4.5°	-0.1162	-0.4162	-2.2569
		Torque $T$		
		-11.264	-14.739	-39.844

TABLE 4A

CALCULATED  $f$  AND  $T$  FOR THE ROTATION OF FINITE DISCS FOR  $N=50$ 

$\gamma_j = 90^\circ$ (flat end, $z = \alpha$ )		$\alpha = 10$	$\alpha = 100$
$i$	$\varphi_j$	stress distribution $f$	
1	$0.9^\circ$	-0.0002	+1.6896
5	$8.1^\circ$	-0.1571	-0.1410
10	$17.1^\circ$	-0.3266	-0.3228
15	$26.1^\circ$	-0.4843	-0.4825
20	$35.1^\circ$	-0.6242	-0.6230
25	$44.1^\circ$	-0.7397	-0.7387
30	$53.1^\circ$	-0.8236	-0.8226
35	$62.1^\circ$	-0.8661	-0.8654
40	$71.1^\circ$	-0.8533	-0.8545
45	$80.1^\circ$	-0.7524	-0.7503
50	$89.1^\circ$	-0.1755	+0.1927

TABLE 4B

CALCULATED  $f$  AND  $T$  FOR THE ROTATION OF FINITE DISCS FOR  $N=50$ 

$\varphi_j=90^\circ$ (curved side, $\rho=1$ )		$\alpha=10$	$\alpha=100$
$i$	$\gamma_j$	stress distribution $f$	
51	89.1°	-1.6759	-8.1545
55	81.9°	-4.2000	-29.988
60	72.9°	-6.7688	-59.289
65	63.9°	-9.3580	-88.152
70	54.9°	-11.861	-115.07
75	45.9°	-14.161	-139.21
80	36.9°	-16.165	-159.94
85	27.9°	-17.803	-176.75
90	18.9°	-19.024	-189.21
95	9.9°	-19.792	-197.02
100	0.9°	-20.081	-199.99
		Torque $T$	
		-267.55	-2529.4

As we pointed out at the beginning of this section, the substitution (3.15) is chosen in view of the known asymptotic behavior of the stress distribution for an infinitesimally thin disc, and thus will not be the 'best' choice for a finite disc also. In fact, one would expect intuitively that the singularity at the edge of a finite disc with an aspect ratio of, say, unity, should be weaker than that of a thin disc. In support of this contention, we note that the calculated values of  $f$  (from table 3) actually decrease towards the edge. To estimate the actual strength of the singularity, a numerical experiment can be attempted by letting

$$f(\rho, \alpha) = \sigma(\rho, \alpha)(1 - \rho^2)^m$$

$$f(1, z) = \sigma(1, z)(\alpha^2 - z^2)^n$$

The values of  $m, n$  are then varied and an estimate of the 'optimal' values may be obtained. The criteria for choosing is that, at those values of  $m, n$ , the corresponding stress distribution  $f$  should approach a finite asymptotic limit as the edge of the disc is approached. Our results are shown in Table 5. To the accuracy of our calculations, it appears that approximately  $m=0.35, n=0.30$  will give the desired result. We should also add that the values of  $\sigma$  calculated for all combinations of  $m, n$  are essentially the same, which will indicate that our calculations are correct.

TABLE 5

CALCULATED VALUES OF  $f$  AS A FUNCTION OF  $m$ ,  $n$ . ( $\alpha=1, N=10$ )

$(\varphi_j, \gamma_j)$	$m=0.5$	$m=0.4$	$m=0.4$	$m=0.3$	$m=0.35$
	$n=0.5$	$n=0.5$	$n=0.4$	$n=0.3$	$n=0.30$
$(4.5^\circ, 90.0^\circ)$	-0.0948	-0.0948	-0.0947	-0.0947	-0.0947
$(13.5^\circ, 90.0^\circ)$	-0.2645	-0.2659	-0.2658	-0.2672	-0.2665
$(22.5^\circ, 90.0^\circ)$	-0.4307	-0.4373	-0.4373	-0.4440	-0.4406
$(31.5^\circ, 90.0^\circ)$	-0.5813	-0.5998	-0.5997	-0.6187	-0.6091
$(40.5^\circ, 90.0^\circ)$	-0.7101	-0.7496	-0.7495	-0.7911	-0.7700
$(49.5^\circ, 90.0^\circ)$	-0.8100	-0.8825	-0.8823	-0.9610	-0.9208
$(58.5^\circ, 90.0^\circ)$	-0.8726	-0.9928	-0.9926	-1.1288	-1.0585
$(67.5^\circ, 90.0^\circ)$	-0.8856	-1.0721	-1.0720	-1.2969	-1.1792
$(76.5^\circ, 90.0^\circ)$	-0.8362	-1.1138	-1.1095	-1.4688	-1.2748
$(85.5^\circ, 90.0^\circ)$	-0.5507	-0.9481	-0.9871	-1.7201	-1.3241
$(90.0^\circ, 85.5^\circ)$	-0.5796	-0.6003	-1.0354	-1.8005	-1.7793
$(90.0^\circ, 76.5^\circ)$	-0.9943	-0.9916	-1.3223	-1.7548	-1.7575
$(90.0^\circ, 67.5^\circ)$	-1.2436	-1.2435	-1.5068	-1.8246	-1.8245
$(90.0^\circ, 58.5^\circ)$	-1.4736	-1.4735	-1.6776	-1.9093	-1.9093
$(90.0^\circ, 49.5^\circ)$	-1.6805	-1.6804	-1.8318	-1.9964	-1.9964
$(90.0^\circ, 40.5^\circ)$	-1.8624	-1.8624	-1.9671	-2.0774	-2.0774
$(90.0^\circ, 31.5^\circ)$	-2.0151	-2.0151	-2.0802	-2.1471	-2.1471
$(90.0^\circ, 22.5^\circ)$	-2.1340	-2.1340	-2.1679	-2.2020	-2.2020
$(90.0^\circ, 13.5^\circ)$	-2.2155	-2.2155	-2.2277	-2.2398	-2.2398
$(90.0^\circ, 4.5^\circ)$	-2.2569	-2.2569	-2.2581	-2.2591	-2.2591

## 4.0 APPLICATION

As mentioned earlier, the torque on the rotating disc and the velocity distribution of the fluid are of interest to us. The former has been calculated in the last chapter. Here we will calculate the velocity fields for several values of  $\alpha$ . Then, the numerical torque values of the last chapter will be compared with an ad hoc equation which we suggested in chapter 2.

### 4.1 Velocity Field

To calculate the velocity field of the fluid for the case of a rotating finite disc with arbitrary aspect ratio  $\alpha$ , we use equation (2.11) which can be written as

$$v(\rho, z) = - \frac{1}{2} \left\{ \int_0^1 \int_0^\infty J_1(\lambda\rho) J_1(\lambda\rho') (e^{-\lambda|z-\alpha|} + e^{-\lambda|z+\alpha|}) d\lambda \sigma(\rho', \alpha) \rho' d\rho' \right. \\ \left. + \int_0^\alpha \int_0^\infty J_1(\lambda\rho) J_1(\lambda) (e^{-\lambda|z-z'|} + e^{-\lambda|z+z'|}) d\lambda \sigma(1, z') dz' \right\} \quad (4.1)$$

Since the stress distribution is obtained only at discrete points on the particle's surface, it is obvious that the same numerical approximations that were introduced in chapter 3 must be followed in this case to yield

$$v(\rho, z) = \frac{-1}{2\pi} \left\{ \sum_{j=1}^N f(\sin\varphi_j, \alpha) \int_{\delta_j} \left( \frac{\sin\theta}{\rho} \right)^{1/2} \right.$$

$$\left\{ Q_{1/2} \left[ \frac{(z-\alpha)^2 + \rho^2 + \sin^2 \theta}{2\rho \sin \theta} \right] + Q_{1/2} \left[ \frac{(z+\alpha)^2 + \rho^2 + \sin^2 \theta}{2\rho \sin \theta} \right] \right\} d\theta$$

$$+ \sum_{j=1}^N f(1, \alpha \sin \gamma_j) \int_{\epsilon_j} \frac{1}{\rho} (-)^{1/2}$$

$$\left\{ Q_{1/2} \left[ \frac{(z-\alpha \sin \beta)^2 + \rho^2 + 1}{2\rho} \right] + Q_{1/2} \left[ \frac{(z+\alpha \sin \beta)^2 + \rho^2 + 1}{2\rho} \right] \right\} d\beta$$

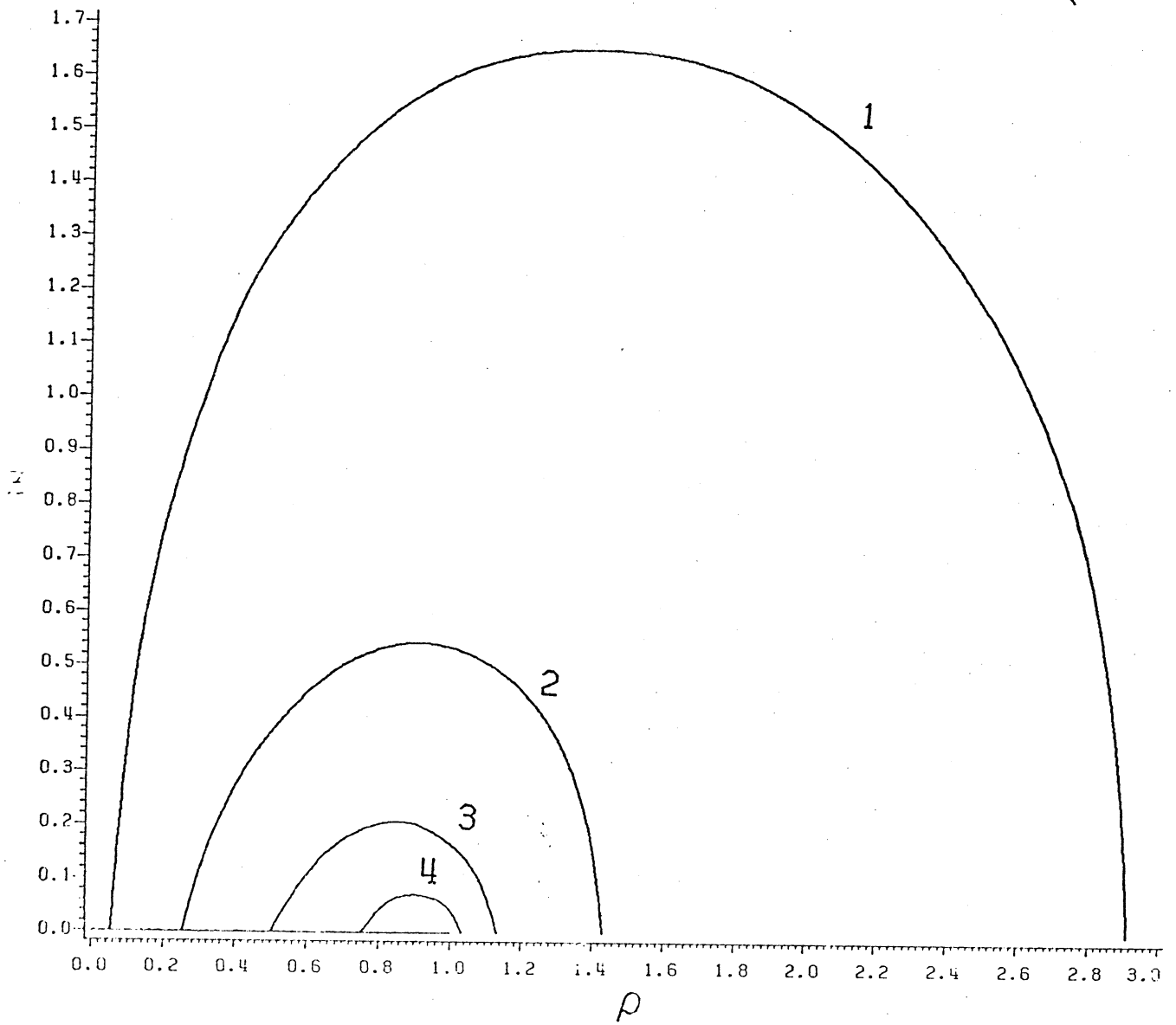
(4.2)

Each line integral may now be calculated and the velocity distribution is then obtained. We have plotted these results in figure 1 ( $\alpha = 0$ ) and figure 2 ( $\alpha = 1$ ). The velocity distributions are clearly consistent with what are expected.

#### 4.2 Torque Comparison

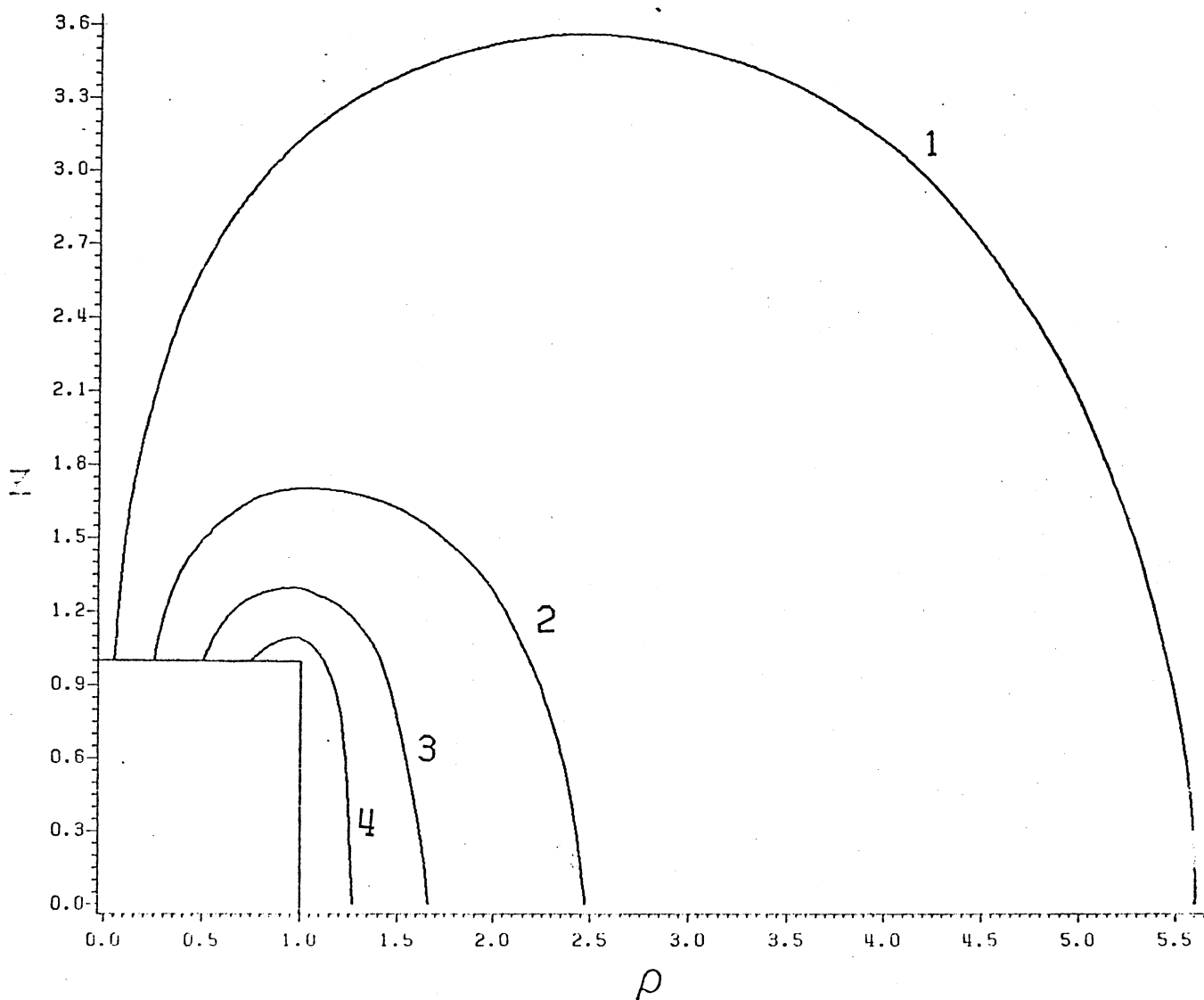
The torque values calculated in chapter 3 are plotted in figure 3 together with the prediction of an ad hoc equation that we suggested (i.e. equation (2.23)). It can be seen that the numerical values are always slightly larger than those obtained from equation (2.23). For the limiting cases (i.e.  $\alpha = 0$  and  $\alpha \rightarrow \infty$ ), however, the discrepancies are very small, which is to be expected. In all cases, equation (2.23), although not rigorously justifiable, is an adequate approximation for the torque on the rotating particle.

FIG 1. VELOCITY FIELD DUE TO THE ROTATION OF A THIN DISC ( $\alpha = 0$ )



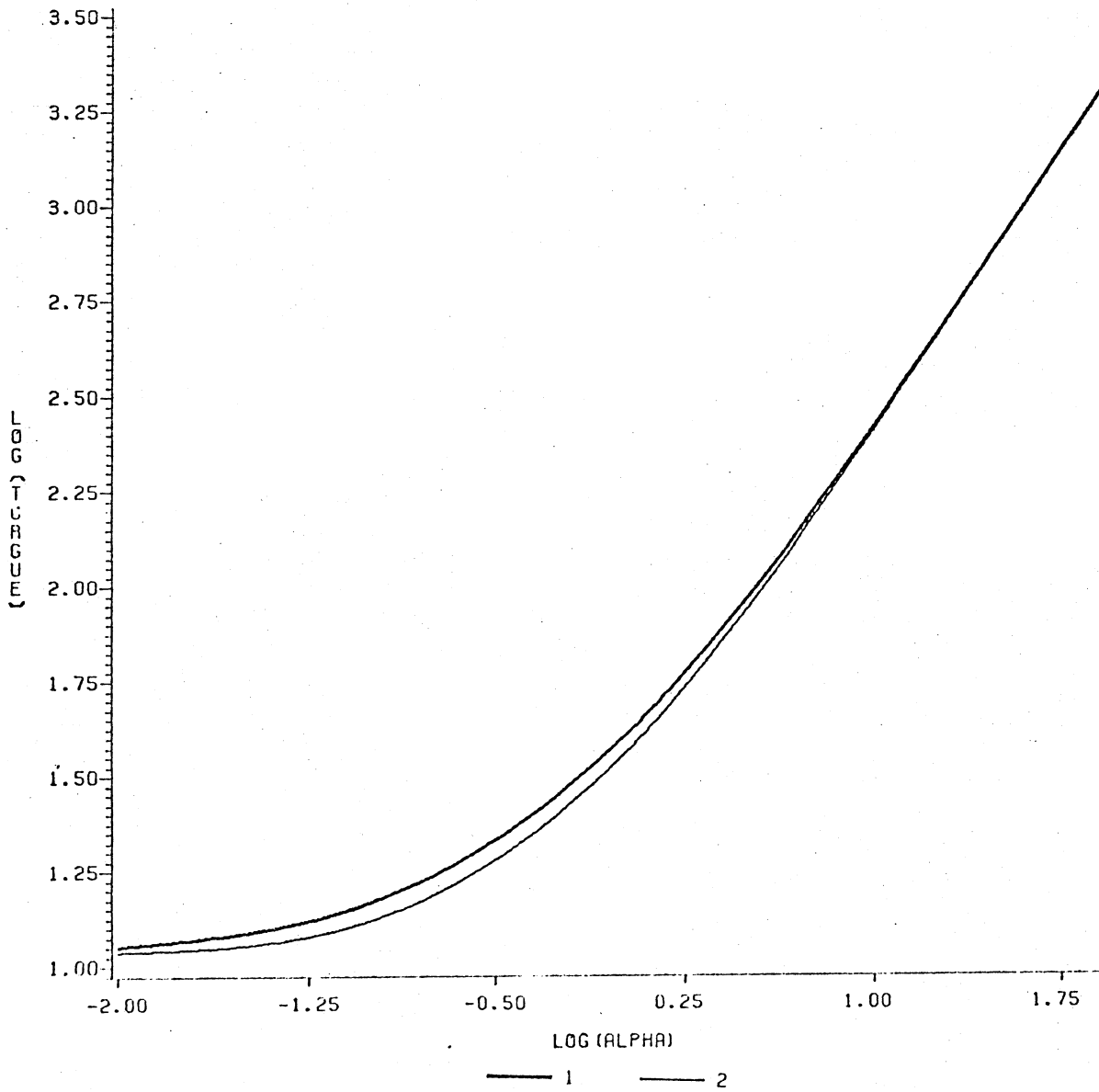
CURVE 1 VELOCITY = 0.05  
CURVE 2 VELOCITY = 0.25  
CURVE 3 VELOCITY = 0.50  
CURVE 4 VELOCITY = 0.75

FIG 2. VELOCITY FIELD DUE TO THE ROTATION OF A FINITE DISC ( $\alpha = 1$ )



CURVE 1 VELOCITY = 0.05  
CURVE 2 VELOCITY = 0.25  
CURVE 3 VELOCITY = 0.50  
CURVE 4 VELOCITY = 0.75

FIGURE 3. THE COMPARISON OF NUMERICAL RESULTS WITH EQUATION (2.23)



CURVE 1 TORQUES FROM NUMERICAL TECHNIQUES  
CURVE 2 TORQUES FROM EQUATION (2.23)

## 5.0 RECOMMENDATIONS AND CONCLUSIONS

This work is part of an ongoing effort to study the slow motion of rigid particles in a viscous fluid by numerical techniques. Here, we have considered the axial rotation of an axisymmetrical particle in an inertialess unbounded Newtonian fluid. By using the method of Green's function, we can obtain a line integral which makes the problem easier to solve. Although there are singularities in the integrand, these can be 'removed' and thus numerical solution of the integral equation is relatively straightforward. From the numerically calculated stress distribution, the velocity field and the torque on the particle can also be obtained. Overall our method is easy to apply and produces very accurate results even for the case of a finite circular cylinder where no analytical solutions presently exist.

As was mentioned at the beginning of this thesis, the method that is developed here may be applied to other problems in mathematical physics, as well as other types of rigid particle motion in a viscous fluid such as the translational motion of a finite circular cylinder. These should be the areas of future research work.

## 6.0 REFERENCES

- Abramowitz, M. and Stegun, I. A. (1970), Handbook of Mathematical Functions, 9th Edition. Dover Publication, INC.
- Batchelor, G. K. (1970), J. Fluid Mech. 44, 419.
- Bowen, B. D. and Masliyah, J. H. (1973), Can. J. Chem. Engr. 51, 8.
- Broersma, S. (1960), J. Chem. Phys. 32, 1632.
- Brunn, P. (1980), J. non-Newt. Fluid Mech. 7, 271.
- Burgers, J. M. (1938), Second Report on Viscosity and Plasticity. Kon. Ned. Akad. Wet., Verhand. 16, 113.
- Caswell, B. (1977), The Mechanics of Viscoelastic Fluids, Appl. Mech. Div., Vol. 22, A.S.M.E.
- Chang, Y. P., Kang, C. S. and Chen, D. J. (1973), Int. J. Heat and Mass Transfer 16, 1905.
- Chwang, A. T. and Wu, T. Y. (1975), J. Fluid Mech. 67, 787.
- Collins, W. D. (1963), Mathematika 10, 72.
- Cooley, M. D. A. and O'Neill, M. E. (1969), Proc. Camb. Phil. Soc. 66, 407.
- Copson, E. T. (1945), Proc. Edinb. Math. Soc. (2), 8, 14-19.
- Cox, R. G. (1970), J. Fluid Mech. 44, 791.
- Cox, R. G. (1971), J. Fluid Mech. 45, 625.
- Cruse, T. A. (1969), Int. J. Solids Struct. 5, 1259.
- Dorrepaal, J. M., O'Neill, M. E. and Ranger, K. B. (1976), J. Fluid Mech. 75, 271.
- Gluckman, M. J., Weinbaum, S. and Pfeffer, R. (1972), J. Fluid Mech. 55, 677.
- Goren, S. L. and O'Neill, M. E. (1980), J. Fluid Mech. 101, 97.
- Gupta, S. C. (1957), ZAMP 8(17) , 257.
- Hunt, B. H. (1968), J. Fluid Mech. 31, 361.
- Jeffrey, G. B. (1915), London Math. Soc. 14, 327.
- Jeffrey, G. B. (1922), Proc. Roy. Soc. A102, 161.

- Kanwall, R. P. (1961), J. Fluid Mech. 10, 17.
- Kirchhoff, G. (1869), J. Reine Angew. Math. 70, 289.
- Leal, L. G. (1979), J. non-Newt. Fluid Mech. 5, 33.
- Leal, L. G. (1980), Ann. Rev. Fluid Mech. 12, 435.
- Majumdar, S. R. and O'Neill, M. E. (1977), ZAMP 28, 541.
- Oberbeck, A. (1876), J. Reine Angew. Math. 81, 62.
- Payne, L. E. and Pell, W. H. (1960), J. Fluid Mech. 7, 529.
- Ray, M. (1936), Phil. Mag. 21 (7), 553.
- Smith, A. M. O. and Hess, J. L. (1966), Prog. Aero. Sci. 8, 1.
- Shail, R. (1979), Int. J. Multiphase Flows 5, 169.
- Stimson, M. and Jeffrey, G. B. (1926), Proc. Roy. Soc. A111, 110.
- Stokes, G. G. (1851), Trans. Camb. Phil. Soc. 9, 8.
- Tillett, J. P. K. (1970), J. Fluid Mech. 44, 401.
- Watson, G. N. (1966), A Treatise on the Theory of Bessels Function,  
2nd Edition. Cambridge University Press.
- Youngren, G. K. and Acrivos, A. (1975), J. Fluid Mech. 69, 377.

APPENDIX A

FORTRAN program for calculating the numerical stress  
distribution and torque of the rotating thin disc  
-----

```
IMPLICIT REAL*8 (A-H,O-Z)
DIMENSION THETA(100),PHI(100),X(100,100),V(100),VE(100),E(100)
DIMENSION XX(100,100),WKAREA(11000)
EXTERNAL Z
COMMON B,C
N=10
WRITE (6,10) N
10 FORMAT (1H1,6X,'NUMBER OF INTERVALS=',I3)
P=3.14159
PHI1=0.
PHI2=P/2.
AA=N
DPHI=(PHI2-PHI1)/AA
I=1
PHI(1)=PHI1+DPHI/2.
THETA(1)=PHI(1)
1 I=I+1
PHI(I)=PHI(I-1)+DPHI
THETA(I)=PHI(I)
IF (I.LT.N) GO TO 1
DO 2 I=1,N
C=PHI(I)
B=DSIN(C)
```

```

DO 3 J=1,N
F1=THETA(J)
DIFF=DABS(F1-C)
IF (I.EQ.J) GO TO 4
X(I,J)=(DCADRE(Z,F1-DPHI/2.,F1+DPHI/2.,1.0D-5,0.00001,ERROR
1,IER)+(DIFF-DPHI/2.)*DLOG(DIFF-DPHI/2.)-(DIFF+DPHI/2.)*DLO
2G(DIFF+DPHI/2.)+DPHI*(DLOG(8.*DTAN(C))-1.))*2./P
GO TO 5
4 X(I,J)=((DCADRE(Z,F1-DPHI/2.,F1,1.0D-5,0.00001,ERROR
1,IER)+DCADRE(Z,F1,F1+DPHI/2.,1.0D-5,0.00001,ERROR,I
2ER))+DPHI*(DLOG(16.*DTAN(C)/DPHI)-1.))*2./P
5 XX(I,J)=X(I,J)
3 CONTINUE
VE(I)=B*(-4./P)
V(I)=B
2 CONTINUE
CALL LEQT2F(XX,1,N,100,V,4,WKAREA,IER)
T=0.
I=0
PHIU=0.
FUNCU=0.
9 I=I+1
PHIL=PHIU
FUNCL=FUNCU
PHIU=PHIL+DPHI
FUNCU=FINTG(PHIU)
T=T+V(I)*(FUNCU-FUNCL)

```

```

V(I)=V(I)*(-2.)
E(I)=V(I)/VE(I)-1.0
IF (I.LT.N) GO TO 9
T=-8.*P*T
TE=-10.666666667
E2=T/TE-1.0
WRITE (6,30) ((X(I,J),I=1,N),J=1,N)
30 FORMAT (5E15.5)
WRITE (6,12)
12 FORMAT (1H0,15X,'STRESS')
WRITE (6,11)
11 FORMAT (2X,'CALCULATED',5X,'EXACT',7X,'ERROR')
WRITE (6,6) (V(I),VE(I),E(I),I=1,N)
6 FORMAT (' ',3E12.5)
WRITE (6,13)
13 FORMAT (1H0,15X,'TORQUE')
WRITE (6,11)
WRITE (6,6) T,TE,E2
STOP
END
DOUBLE PRECISION FUNCTION Z(A)
IMPLICIT REAL*8 (A-H,O-Z)
COMMON B,C
Z=0.
IF (DABS(A-C).LT.1.0D-7) GO TO 1
IF (DABS(A).LT.1.0D-7) GO TO 2
X=DSIN(A)

```

```

Y=B
PP=(X**2+Y**2)/2./X/Y
QQ=DSQRT(X*Y)*2./(X+Y)
RR=((X-Y)/(X+Y))**2
RR2=RR*RR
RR3=RR2*RR
RR4=RR3*RR
ARR=DLOG(RR)
AK=1.3862944+0.0966634*RR+0.0359009*RR2+0.0374256*RR3+0.0
114512*RR4-(0.5+0.1249859*RR+0.0688025*RR2+0.0332836*RR3+0
2.0044179*RR4)*ARR
AE=1.0+0.4432514*RR+0.062606*RR2+0.0475738*RR3+0.0173651*
1RR4-(0.2499837*RR+0.0920018*RR2+0.040697*RR3+0.0052645*RR
24)*ARR
Z=DSQRT(X/Y)*(PP*QQ*AK-2./QQ*AE)
2 Z=Z+DLOG(DABS(A-C)/8./DTAN(C))+2.
1 RETURN
END
DOUBLE PRECISION FUNCTION FINTG(A)
IMPLICIT REAL*8 (A-H,O-Z)
X=DSIN(A)
Y=DCOS(A)
FINTG=(A-X*Y)/2.
RETURN
END

```

## APPENDIX B

FORTRAN program for calculating the numerical stress  
distribution and torque of the rotating finite disc  
-----

```
      IMPLICIT REAL*8 (A-H,O-Z)
      DIMENSION THETA(100),PHI(100),X(100,100),V(100)
      DIMENSION WKAREA(11000),BETA(100),GAMA(100)
      EXTERNAL Z,Z1,Z2,Z3,Z4,Z5,Z6,Z7
      COMMON B,C,ALPHA,E,F
      N=50
      WRITE (6,10) N
10    FORMAT (6X,'NUMBER OF INTERVALS=',I3/)
      ALPHA=10.0
      WRITE (6,14) ALPHA
14    FORMAT (15X,'ALPHA=',F7.2/)
      P=3.14159
      PHI1=0.
      GAMA1=0.
      PHI2=P/2.
      GAMA2=P/2.
      N2=N*2
      DPHI=(PHI2-PHI1)/N
      DGAMA=(GAMA2-GAMA1)/N
      I=1
      PHI(1)=PHI1+DPHI/2.
      GAMA(1)=GAMA1+DGAMA/2.
```

```

    THETA(1)=PHI(1)
    BETA(1)=GAMA(1)
1  I=I+1
    PHI(I)=PHI(I-1)+DPHI
    GAMA(I)=GAMA(I-1)+DGAMA
    THETA(I)=PHI(I)
    BETA(I)=GAMA(I)
    IF (I.LT.N) GO TO 1
    DO 2 I=1,N
    C=PHI(I)
    B=DSIN(C)
    DO 3 J=1,N
    F1=THETA(J)
    DIFF=DABS(F1-C)
    IF (I.EQ.J) GO TO 4
    X(I,J)=DCADRE(Z,F1-DPHI/2.,F1+DPHI/2.,1.0D-5,0.00001,ERROR
1,IER)+(DIFF-DPHI/2.)*DLOG(DIFF-DPHI/2.)-(DIFF+DPHI/2.)*DLOG
2(DIFF+DPHI/2.)+DPHI*(DLOG(8.*DTAN(C))-1.)+DCADRE(Z1,F1-
3DPHI/2.,F1+DPHI/2.,1.0D-5,0.00001,ERROR,IER)
    GO TO 3
4  X(I,J)=DCADRE(Z,F1-DPHI/2.,F1,1.0D-5,0.00001,ERROR
1,IER)+DCADRE(Z,F1,F1+DPHI/2.,1.0D-5,0.00001,ERROR,I
2ER)+DPHI*(DLOG(16.*DTAN(C)/DPHI)-1.)+DCADRE(Z1,F1-DPHI/2.,
3F1+DPHI/2.,1.0D-5,0.00001,ERROR,IER)
3  CONTINUE
    V(I)=B
    V(I+N)=1.

```

```

2 CONTINUE
  DO 22 I1=1,N
    C=PHI(I1)
    B=DSIN(C)
    DO 22 J1=1,N
      G1=BETA(J1)
      X(I1,N2+1-J1)= DCADRE(Z2,G1-DGAMA/2.,G1+DGAMA/2.,1.0D-5,0.00001,
1ERROR,IER)+DCADRE(Z3,G1-DGAMA/2.,G1+DGAMA/2.,1.0D-5,0.00001,
2ERROR,IER)
22 CONTINUE
  DO 24 I2=1,N
    E=GAMA(I2)
    F=DSIN(E)
    DO 24 J2=1,N
      G2=THETA(J2)
      X(N2+1-I2,J2)=DCADRE(Z4,G2-DPHI/2.,G2+DPHI/2.,1.0D-5,0.00001,
1ERROR,IER)+DCADRE(Z5,G2-DPHI/2.,G2+DPHI/2.,1.0D-5,0.00001,
2ERROR,IER)
24 CONTINUE
  DO 25 I3=1,N
    E=GAMA(I3)
    F=DSIN(E)
    DO 26 J3=1,N
      G3=BETA(J3)
      DIFF1=DABS(G3-E)
      IF (I3.EQ.J3) GO TO 27
      X(N2+1-I3,N2+1-J3)=DCADRE(Z6,G3-DGAMA/2.,G3+DGAMA/2.,1.0D-5,

```

```

10. 00001, ERROR, IER) - (DIFF1 + DGAMA/2.) * DLOG(DIFF1 + DGAMA/2.) + (DIFF1 -
2DGAMA/2.) * DLOG(DIFF1 - DGAMA/2.) + DGAMA * (DLOG(8./ALPHA/DCOS(E)) - 1) +
3DCADRE(Z7, G3 - DGAMA/2., G3 + DGAMA/2., 1.0D-5, 0.00001, ERROR, IER)

GO TO 26

27 X(N2+1-I3, N2+1-J3) = DCADRE(Z6, G3 - DGAMA/2., G3, 1.0D-5, 0.00001, ERROR,
1 IER) + DCADRE(Z6, G3, G3 + DGAMA/2., 1.0D-5, 0.00001, ERROR, IER) - DGAMA *
2 (DLOG(ALPHA * DCOS(E) * DGAMA/16.) + 1) + DCADRE(Z7, G3 - DGAMA/2.,
3 G3 + DGAMA/2., 1.0D-5, 0.00001, ERROR, IER)

26 CONTINUE

25 CONTINUE

CALL LEQT2F(X, 1, N2, 100, V, 4, WKAREA, IER)

T = 0.

I = 0

PHIU = 0.

GAMAU = 0.

FUNCU = 0.

FUNU = 0.

9 I = I + 1

PHIL = PHIU

GAMAL = GAMAU

FUNCL = FUNCU

FUNL = FUNU

PHIU = PHIL + DPHI

GAMAU = GAMAL + DGAMA

FUNCU = FINTG(PHIU)

FUNU = FIN(GAMAU)

V(I) = V(I) * (-2.) * P

```

```

V(N2+1-I)=V(N2+1-I)*(-2.)*P
T=T+V(I)*(FUNCU-FUNCL)+V(N2+1-I)*(FUNU-FUNL)
IF (I.LT.N) GO TO 9
T=4.*P*T
WRITE (6,12)
12 FORMAT (15X,'STRESS'/)
WRITE (6,15) (V(I),I=1,N2)
15 FORMAT (6E12.5/)
WRITE (6,13)
13 FORMAT (15X,'TORQUE'/)
WRITE (6,16) T
16 FORMAT (15X,E12.5)
STOP
END
DOUBLE PRECISION FUNCTION Z(A)
IMPLICIT REAL*8 (A-H,O-Z)
COMMON B,C,ALPHA,E,F
Z=0.
IF (DABS(A-C).LT.1.0D-7) GO TO 1
IF (DABS(A).LT.1.0D-7) GO TO 2
X=DSIN(A)
Y=B
PP=(X**2+Y**2)/2./X/Y
QQ=DSQRT(X*Y)*2./(X+Y)
RR=((X-Y)/(X+Y))**2
RR2=RR*RR
RR3=RR2*RR

```

```

RR4=RR3*RR
ARR=DLOG(RR)
AK=1.3862944+0.0966634*RR+0.0359009*RR2+0.0374256*RR3+0.0
114512*RR4-(0.5+0.1249859*RR+0.0688025*RR2+0.0332836*RR3+0
2.0044179*RR4)*ARR
AE=1.0+0.4432514*RR+0.062606*RR2+0.0475738*RR3+0.0173651*
1RR4-(0.2499837*RR+0.0920018*RR2+0.040697*RR3+0.0052645*RR
24)*ARR
Z=DSQRT(X/Y)*(PP*QQ*AK-2./QQ*AE)
2 Z=Z+DLOG(DABS(A-C)/8./DTAN(C))+2.
1 RETURN
END
DOUBLE PRECISION FUNCTION Z1(A)
IMPLICIT REAL*8 (A-H,O-Z)
COMMON B,C,ALPHA,E,F
Z1=0.
IF (DABS(A).LT.1.0D-7) GO TO 2
A1=ALPHA
X=DSIN(A)
Y=B
PP=(X**2+Y**2+4*A1**2)/2/X/Y
QQ=2*DSQRT(X*Y/(4*A1**2+(X+Y)**2))
RR=((X-Y)**2+4*A1**2)/((X+Y)**2+4*A1**2)
RR2=RR*RR
RR3=RR2*RR
RR4=RR3*RR
ARR=DLOG(RR)

```

```

      AK=1.3862944+0.0966634*RR+0.0359009*RR2+0.0374256*RR3+0.0
114512*RR4-(0.5+0.1249859*RR+0.0688025*RR2+0.0332836*RR3+0
2.0044179*RR4)*ARR

      AE=1.0+0.4432514*RR+0.062606*RR2+0.0475738*RR3+0.0173651*
1RR4-(0.2499837*RR+0.0920018*RR2+0.040697*RR3+0.0052645*RR
24)*ARR

      Z1=DSQRT(X/Y)*(PP*QQ*AK-2./QQ*AE)
2 RETURN

      END

      DOUBLE PRECISION FUNCTION Z2(A)

      IMPLICIT REAL*8 (A-H,O-Z)

      COMMON B,C,ALPHA,E,F

      Z2=0.

      IF (DABS(A).LT.1.0D-7) GO TO 2

      A1=ALPHA

      X=DSIN(A)

      Y=B

      PP=(A1**2*(1.-X)**2+Y**2+1.)/2./Y

      QQ=2*DSQRT(Y/(A1**2*(1.-X)**2+(Y+1)**2))

      RR=(A1**2*(1.-X)**2+(Y-1. )**2)/(A1**2*(1.-X)**2+(Y+1. )**2)

      RR2=RR*RR

      RR3=RR2*RR

      RR4=RR3*RR

      ARR=DLOG(RR)

      AK=1.3862944+0.0966634*RR+0.0359009*RR2+0.0374256*RR3+0.0
114512*RR4-(0.5+0.1249859*RR+0.0688025*RR2+0.0332836*RR3+0
2.0044179*RR4)*ARR

```

```

      AE=1.0+0.4432514*RR+0.062606*RR2+0.0475738*RR3+0.0173651*
1RR4-(0.2499837*RR+0.0920018*RR2+0.040697*RR3+0.0052645*RR
24)*ARR
      Z2=DSQRT(1./Y)*(PP*QQ*AK-2./QQ*AE)
2 RETURN
      END
      DOUBLE PRECISION FUNCTION Z3(A)
      IMPLICIT REAL*8 (A-H,O-Z)
      COMMON B,C,ALPHA,E,F
      Z3=0.
      IF (DABS(A).LT.1.0D-7) GO TO 2
      A1=ALPHA
      X=DSIN(A)
      Y=B
      PP=(A1**2*(1.+X)**2+Y**2+1.)/2./Y
      QQ=2*DSQRT(Y/(A1**2*(1.+X)**2+(Y+1)**2))
      RR=(A1**2*(1.+X)**2+(Y-1.))**2/(A1**2*(1.+X)**2+(Y+1.))**2)
      RR2=RR*RR
      RR3=RR2*RR
      RR4=RR3*RR
      ARR=DLOG(RR)
      AK=1.3862944+0.0966634*RR+0.0359009*RR2+0.0374256*RR3+0.0
114512*RR4-(0.5+0.1249859*RR+0.0688025*RR2+0.0332836*RR3+0
2.0044179*RR4)*ARR
      AE=1.0+0.4432514*RR+0.062606*RR2+0.0475738*RR3+0.0173651*
1RR4-(0.2499837*RR+0.0920018*RR2+0.040697*RR3+0.0052645*RR
24)*ARR

```

```

      Z3=DSQRT(1./Y)*(PP*QQ*AK-2./QQ*AE)
2  RETURN
      END
      DOUBLE PRECISION FUNCTION Z4(A)
      IMPLICIT REAL*8 (A-H,O-Z)
      COMMON B,C,ALPHA,E,F
      Z4=0.
      IF (DABS(A).LT.1.0D-7) GO TO 2
      A1=ALPHA
      X=DSIN(A)
      Y=F
      PP=(A1**2*(Y-1.)**2+X**2+1.)/2./X
      QQ=2*DSQRT(X/(A1**2*(Y-1.)**2+(X+1)**2))
      RR=(A1**2*(Y-1.)**2+(X-1.)**2)/(A1**2*(Y-1.)**2+(X+1.)**2)
      RR2=RR*RR
      RR3=RR2*RR
      RR4=RR3*RR
      ARR=DLOG(RR)
      AK=1.3862944+0.0966634*RR+0.0359009*RR2+0.0374256*RR3+0.0
114512*RR4-(0.5+0.1249859*RR+0.0688025*RR2+0.0332836*RR3+0
2.0044179*RR4)*ARR
      AE=1.0+0.4432514*RR+0.062606*RR2+0.0475738*RR3+0.0173651*
1RR4-(0.2499837*RR+0.0920018*RR2+0.040697*RR3+0.0052645*RR
24)*ARR
      Z4=DSQRT(X)*(PP*QQ*AK-2./QQ*AE)
2  RETURN
      END

```

```

DOUBLE PRECISION FUNCTION Z5(A)
IMPLICIT REAL*8 (A-H,O-Z)
COMMON B,C,ALPHA,E,F
Z5=0.
IF (DABS(A).LT.1.0D-7) GO TO 2
A1=ALPHA
X=DSIN(A)
Y=F
PP=(A1**2*(Y+1.))**2+X**2+1.)/2./X
QQ=2*DSQRT(X/(A1**2*(Y+1.))**2+(X+1)**2))
RR=(A1**2*(Y+1.))**2+(X-1.))**2)/(A1**2*(Y+1.))**2+(X+1.))**2)
RR2=RR*RR
RR3=RR2*RR
RR4=RR3*RR
ARR=DLOG(RR)
AK=1.3862944+0.0966634*RR+0.0359009*RR2+0.0374256*RR3+0.0
114512*RR4-(0.5+0.1249859*RR+0.0688025*RR2+0.0332836*RR3+0
2.0044179*RR4)*ARR
AE=1.0+0.4432514*RR+0.062606*RR2+0.0475738*RR3+0.0173651*
1RR4-(0.2499837*RR+0.0920018*RR2+0.040697*RR3+0.0052645*RR
24)*ARR
Z5=DSQRT(X)*(PP*QQ*AK-2./QQ*AE)
2 RETURN
END
DOUBLE PRECISION FUNCTION Z6(A)
IMPLICIT REAL*8 (A-H,O-Z)
COMMON B,C,ALPHA,E,F

```

```

Z6=0.
IF (DABS(A-E).LT.1.0D-7) GO TO 1
IF (DABS(A).LT.1.0D-7) GO TO 2
A1=ALPHA
X=DSIN(A)
Y=F
PP=(A1**2*(Y-X)**2+2.)/2.
QQ=2*DSQRT(1./(A1**2*(Y-X)**2+4))
RR=(A1**2*(Y-X)**2)/(A1**2*(Y-X)**2+4.)
RR2=RR*RR
RR3=RR2*RR
RR4=RR3*RR
ARR=DLOG(RR)
AK=1.3862944+0.0966634*RR+0.0359009*RR2+0.0374256*RR3+0.0
114512*RR4-(0.5+0.1249859*RR+0.0688025*RR2+0.0332836*RR3+0
2.0044179*RR4)*ARR
AE=1.0+0.4432514*RR+0.062606*RR2+0.0475738*RR3+0.0173651*
1RR4-(0.2499837*RR+0.0920018*RR2+0.040697*RR3+0.0052645*RR
24)*ARR
Z6=(PP*QQ*AK-2./QQ*AE)
2 Z6=Z6-DLOG(8./A1/DCOS(E)/DABS(A-E))+2.
1 RETURN
END
DOUBLE PRECISION FUNCTION Z7(A)
IMPLICIT REAL*8 (A-H,O-Z)
COMMON B,C,ALPHA,E,F
Z7=0.

```

```

IF (DABS(A).LT.1.0D-7) GO TO 1
A1=ALPHA
X=DSIN(A)
Y=F
PP=(A1**2*(Y+X)**2+2.)/2.
QQ=2*DSQRT(1./(A1**2*(Y+X)**2+4))
RR=(A1**2*(Y+X)**2)/(A1**2*(Y+X)**2+4.)
RR2=RR*RR
RR3=RR2*RR
RR4=RR3*RR
ARR=DLOG(RR)
AK=1.3862944+0.0966634*RR+0.0359009*RR2+0.0374256*RR3+0.0
114512*RR4-(0.5+0.1249859*RR+0.0688025*RR2+0.0332836*RR3+0
2.0044179*RR4)*ARR
AE=1.0+0.4432514*RR+0.062606*RR2+0.0475738*RR3+0.0173651*
1RR4-(0.2499837*RR+0.0920018*RR2+0.040697*RR3+0.0052645*RR
24)*ARR
Z7=(PP*QQ*AK-2./QQ*AE)
1 RETURN
END
DOUBLE PRECISION FUNCTION FINTG(A)
IMPLICIT REAL*8 (A-H,O-Z)
X=DSIN(A)
Y=DCOS(A)
FINTG=(A-X*Y)/2.
RETURN
END

```

```
DOUBLE PRECISION FUNCTION FIN(A)
  IMPLICIT REAL*8 (A-H,O-Z)
  FIN=A
  RETURN
END
```

Digitization Information Page

Local identifier        Leu1983

Source information

Format                Book  
Content type        Text  
Source ID            Gift copy from department; not added to MU collection.  
Notes

Capture information

Date captured        June 2023  
Scanner manufacturer Fujitsu  
Scanner model        fi-7460  
Scanning system software ScandAll Pro v. 2.1.5 Premium  
Optical resolution    600 dpi  
Color settings        8 bit grayscale  
File types            tiff  
Notes

Derivatives - Access copy

Compression        Tiff: LZW compression  
Editing software    Adobe Photoshop  
Resolution          600 dpi  
Color                grayscale  
File types            pdf created from tiffs  
Notes                Images cropped, straightened, brightened